

Magnetic and exchange studies in amorphous $\text{Co}_{80-x}\text{Ho}_x\text{B}_{20}$ alloys

O. El Marrakechi¹, A. Kaal¹, S. Sayouri^{1,a}, M. Tlemçani^{1,2}, and H. Lassri³

¹ Laboratoire de Physique Théorique et Appliquée (LPTA), Faculté des Sciences Dhar Mahraz, BP 1796, Fès Atlas, Morocco

² Laboratoire de Physique de la Matière Condensée et de l'Environnement (LPMCE), E.N.S. Fès-Bensouda, Morocco

³ Laboratoire de Physique des Matériaux et de Microélectronique, Université Hassan II, Faculté des Sciences, BP 5366, Aïn Chock, Route d'El Jadida, km-8, Casablanca, Morocco

Received 25 October 2002 / Received in final form 7 June 2003

Published online 9 September 2003 – © EDP Sciences, Società Italiana di Fisica, Springer-Verlag 2003

Abstract. Amorphous $\text{Co}_{80-x}\text{Ho}_x\text{B}_{20}$ alloys were prepared by melt spinning technique and their magnetic properties have been studied. The magnetic compensation occurs at about $x = 8$. Antiferromagnetic coupling between Co and Ho prevails and breaks at relatively high-fields. The mean field theory has been used to explain the temperature dependence of the magnetization. The exchange interactions between Co-Co and Co-Ho atom pairs have been evaluated.

PACS. 75.50.Kj Amorphous and quasicrystalline magnetic materials – 75.30.Et Exchange and superexchange interactions

1 Introduction

Amorphous transition metal (T) rare-earth (R) alloys have been extensively investigated from practical and fundamental points of view [1,2]. First studies related to these alloys have shown that they exhibit several properties: giant coercivity [3], magnetic bubbles [4], etc. Moreover, contrary to their crystalline analogs, amorphous alloys have revealed a great variety of magnetic structures and phase transition, and due to the possibility of their production over a wide range of concentrations, they offer a unique possibility to smoothly modify their basic magnetic parameters.

Amorphous alloys based on R metals with strong spin-orbit interaction also exhibit random anisotropy, which arises from the topological disorder which causes the local symmetry axes to be randomly oriented. As in intermetallics, in amorphous alloys the magnetic moment of the heavy rare-earth couples antiferromagnetically to that of the transition metal. However, under very high magnetic field this coupling breaks down and the field dependence of the magnetization shows very interesting behaviors.

In order to study the influence of Ho addition on the magnetic properties of Co-B alloys, amorphous $\text{Co}_{80-x}\text{Ho}_x\text{B}_{20}$ alloys, with $0 \leq x \leq 12$, were prepared, and their magnetic properties investigated. Thermal variation of magnetization has been analyzed in terms of the mean field theory and the exchange integrals, $J_{\text{Co-Co}}$ and

$J_{\text{Co-Ho}}$ have been deduced. From the high-field magnetization behavior, we have evaluated the molecular field coefficient. Comparison of all these parameters with those corresponding to Fe-Ho-B alloys, has been made.

2 Experimental

Amorphous $\text{Co}_{80-x}\text{Ho}_x\text{B}_{20}$ alloys with $0 \leq x \leq 12$ were prepared by melt spinning technique using a single roller in an argon atmosphere. The amorphous state of the samples was verified by X-ray diffraction. The compositions of the alloys were determined by electron probe microanalysis. Magnetization measurements were performed at 4.2 K in applied fields up to 20 T (at the S.N.C.I., Grenoble). The Curie temperature, T_c , of the a- $\text{Co}_{80-x}\text{Ho}_x\text{B}_{20}$ alloys was determined from the thermomagnetic data.

3 Results and discussion

3.1 Magnetization at 3 T

For all the samples, saturation occurred at about 3 T. The moment of Ho was determined as follows. It is known that with the addition of rare-earth metal, the T moment decreases due to hybridization of the $5d$ and $3d$ orbitals. This decrease in Co moment can be considered as negligible for $x < 5$, as shown for the case of Er [5] and Tm [6]. So for $x = 3.6$, the Co moment can be taken as $1.25 \mu_B$,

^a e-mail: sayouri1@caramail.com, ssayouri@yahoo.com

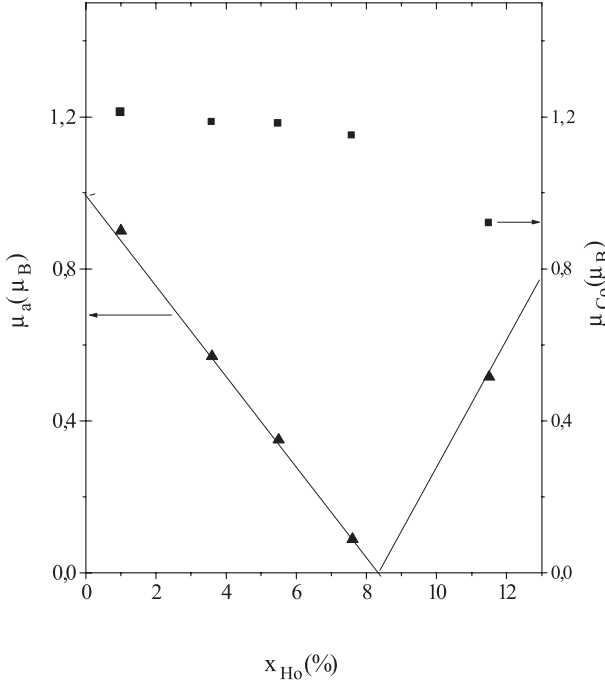


Fig. 1. Concentration dependences of μ_a , the magnetic moment of the a-Co_{80-x}Ho_xB₂₀ alloys (▲), at 8 K, and, μ_{Co} , the magnetic moment of Co (■).

a value which was obtained for the sample with $x = 0$, and which agrees well with the results published [5, 7, 8]. Knowing the alloy moment, μ_a , and using the relation:

$$\mu_a = [(80 - x)\mu_{Co} - x\mu_{Ho}]/100 \quad (1)$$

we calculated μ_{Ho} to be $10.2 \pm 0.5 \mu_B$. This value agrees with the theoretical value (g_J) of $10 \mu_B$ and is close to the experimental value of $10.3 \mu_B$ found in the literature [9]. This would indicate that the Ho spin structure is collinear on the first approximation, and that the random anisotropy of Ho is rather small, although the ground state of trivalent Ho is 5I_8 with a spin-orbit coupling. However, fields of about 3T were necessary to saturate the samples which implies that some anisotropy is present, and therefore that the antiferromagnetic interaction between Co and Ho (J_{Co-Ho}) is stronger than the random anisotropy. Such situation has been observed for Fe-Ho-B alloys [10]. However, in amorphous Co-Er-B alloys the Er spin structure was found to be conical with a large average apex angle of about 82° , which was attributed to the strong random anisotropy of Er [5] and the antiferromagnetic interaction between Co and Er (J_{Co-Er}) which lead to a speromagnetic structure [11].

μ_{Co} for other alloys may now be calculated based on the assumption that μ_{Ho} is independent of x . Figure 1 shows the variation of μ_a with Ho concentration. μ_a decreases rapidly and linearly, as a consequence of an antiferromagnetic coupling of the Co and Ho moments, and the compensation of the moments occurs for about $x = 8$.

The temperature dependence of the magnetic moment of the samples has been studied using the mean-field theory [12] in which the thermal behavior could be described

Table 1. Values of exchange integrals for four concentrations.

x	S_{Co}	T_c^{exp} (K)	J_{Co-Co} (K)	J_{Co-Ho} (K)
3.6	0.56	470	79	10.6
5.5	0.55	465	81.5	10.3
7.6	0.52	435	82.3	11.7
11.5	0.47	370	88	12.4

Table 2. Comparison of exchange integrals (J_{RT}) and the molecular field coefficient, (n_{RT}) relative to Fe-Ho-B [10] and Co-Ho-B (this study) alloys.

Alloys	J_{RT} (K)	n_{RT}
Co _{72.4} Ho _{7.6} B ₂₀	11.8	51.95
Fe _{73.4} Ho _{7.6} B ₁₉	7.8	39.9

by the Brillouin function:

$$\mu_i(T) = \mu_i(0 \text{ K})B_{J_i}(x_i), \quad x_i = \frac{g_i J_i \mu_B H_i}{k_B T} \quad (2)$$

where B_{J_i} , g_i and J_i are respectively the Brillouin function, the Landé factor and the effective total momentum of the ion i , H_i is the molecular field acting on the site i , and the other constants have their usual meaning. The molecular fields H_{Co} and H_{Ho} are expressed as:

$$H_{Co} = \frac{2 J_{Co-Co} z_{Co-Co} S_{Co}(T)}{g_{Co} \mu_B} + \frac{2 J_{Co-Ho} z_{Co-Ho} (g_{Ho} - 1) J_{Ho}(T)}{g_{Co} \mu_B} \quad (3a)$$

$$H_{Ho} = \frac{2 J_{Ho-Co} z_{Ho-Co} (g_{Ho} - 1) S_{Co}(T)}{g_{Ho} \mu_B} + \frac{2 J_{Ho-Ho} z_{Ho-Ho} (g_{Ho} - 1)^2 J_{Ho}(T)}{g_{Ho} \mu_B} \quad (3b)$$

where J_{Co-Co} , J_{Co-Ho} , and J_{Ho-Ho} are the exchange integrals for Co-Co, Co-Ho, and Ho-Ho interactions, respectively, z_{ij} ($i, j = Co, Ho$) is the number of nearest neighbors of the atom j for the atom i . Figure 2 shows the fitting procedure results (in which J_{Ho-Ho} has been neglected), and values of J_{Co-Co} and J_{Co-Ho} , for four concentrations are collected in Table 1. It is seen from this table that J_{Co-Co} increases while J_{Co-Ho} remains practically constant. The calculated exchange integrals, J_{Co-Ho} , are slight larger compared to those, J_{Fe-Ho} , obtained for Fe-Ho-B alloys [10]. Table 2 compares J_{RT} values, for the same concentrations, for Ho-Co-B and Fe-Ho-B alloys [10].

The exchange constant $A(T)$ can be calculated using the following relation [13]:

$$A(T) = n_{Ho-Ho} J_{Ho-Ho} [g_{Ho} - 1]^2 J_{Ho}^2(T) (x/100)^2 / r_{Ho-Ho} + [n_{Co-Ho} + n_{Ho-Co}] J_{Co-Ho} [g_{Ho} - 1] J_{Ho}(T) S_{Co}(T) [x(80 - x)/(100)^2] / r_{Ho-Co} + n_{Co-Co} J_{Co-Co} S_{Co}^2(T) [(80 - x)/100]^2 / r_{Co-Co} \quad (4)$$

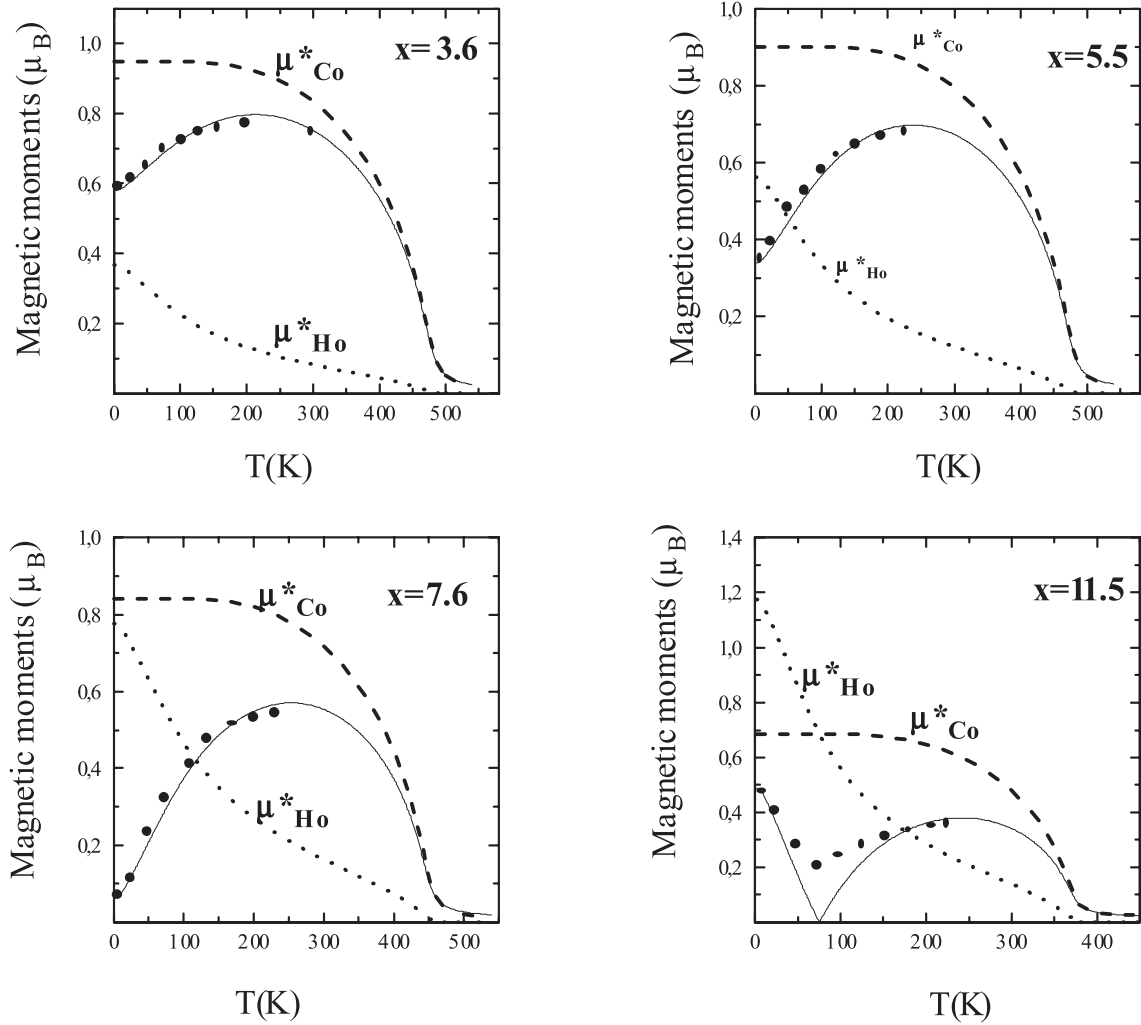


Fig. 2. Temperature dependence of the magnetic moment of the alloys: solid circles: experimental data, solid lines: calculated alloy moment, dashed lines: calculated total Co moment ($\mu_{\text{Co}}^* = ((80 - x)\mu_{\text{Co}}/100)$), dotted lines: calculated total Ho moment ($\mu_{\text{Ho}}^* = x\mu_{\text{Ho}}/100$).

where we have neglected the third term, and where n_{ij} is the number of maximally permissible atom pairs per unit volume extended to first neighbors, taking to be two in our case, r_{ij} are the interatomic distances, which are taken to be $r_{\text{Co-Co}} = 2.5 \text{ \AA}$, $r_{\text{Co-Ho}} = 3 \text{ \AA}$, in accordance with the structural data of Harris *et al.* [14]. Figure 3 shows the temperature dependence of A , for different concentrations. Figure 4 compares the variation of A , at low temperature, as a function of concentration, for Co-Ho-B and Fe-Ho-B [10] alloys; the exchange decreases more rapidly in Fe-Ho-B alloys than in Co-Ho-B ones.

3.2 Magnetization at 4.2 K for $3 \text{ T} < H \leq 20 \text{ T}$

Figure 5 shows the field dependence of the magnetic moment of the alloys, μ_a , for two compositions $x = 3.6$ and $x = 11.5$. It is seen from this Figure that under high applied fields, the magnetization curves exhibit a pronounced magnetic transition, and that the high-field part

of these curves intercepts the μ_a -axis at the same ordinate which is close to zero magnetic field. Furthermore, these curves resemble those of ferrimagnetic compounds (which a schematic representation is given in the inset of Fig. 5), which behavior can be understood on the basis of the two-sublattice model. Indeed, the latter has been applied in the case of amorphous alloys [15–18] and that of intermetallics compounds [19,20]. It is based on the assumption that the magnetization curve can be considered as that expected for an ideal ferrimagnetic system consisting of two well-defined magnetic sublattices coupled by antiferromagnetic interactions. This magnetization curve (Inset of Fig. 5) results from a consideration of the free energy of the ferrimagnetic system [21]

$$E = M_T B - M_R B + n_{RT} M_T M_R. \quad (5)$$

M_T and M_R denote the magnetization of the two sublattices, n_{RT} is the intersublattice molecular field coefficient, which value is a measure of the slope of the magnetization curve observed in intermediate fields. At sufficiently low

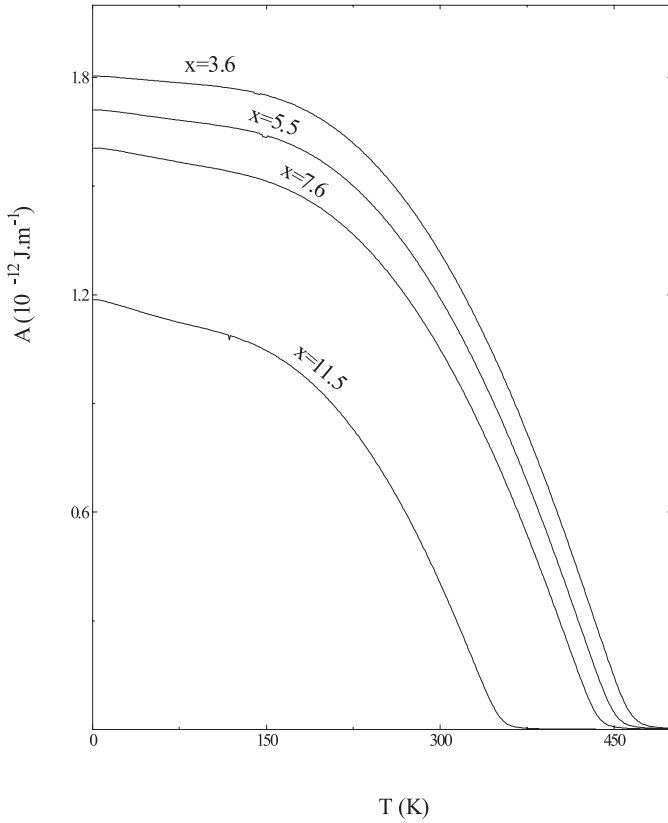


Fig. 3. Temperature dependence of the exchange constant, A , for four concentrations.

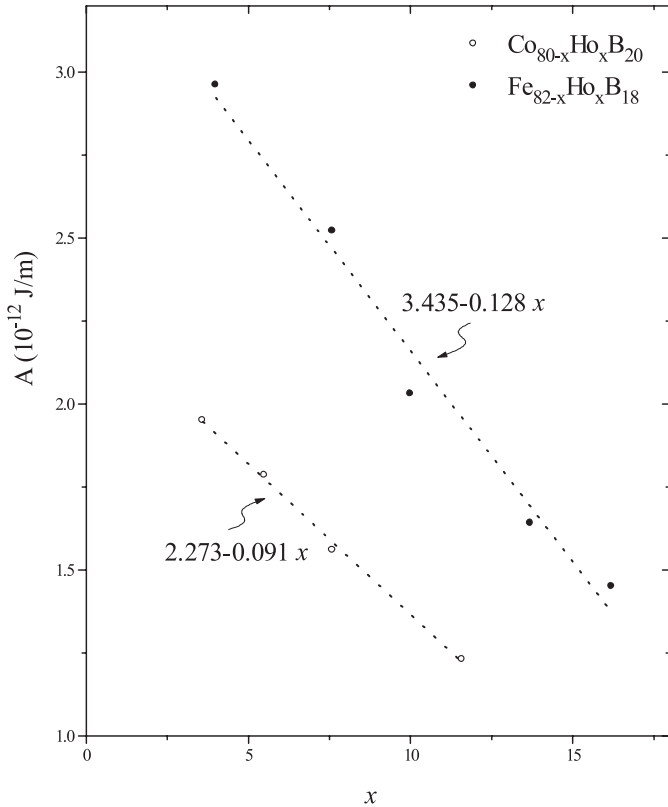


Fig. 4. Concentration dependences of A , at low temperature, for $\text{Co}_{80-x}\text{Ho}_x\text{B}_{20}$ (this study) and $\text{Fe}_{82-x}\text{Ho}_x\text{B}_{18}$ alloys [10].

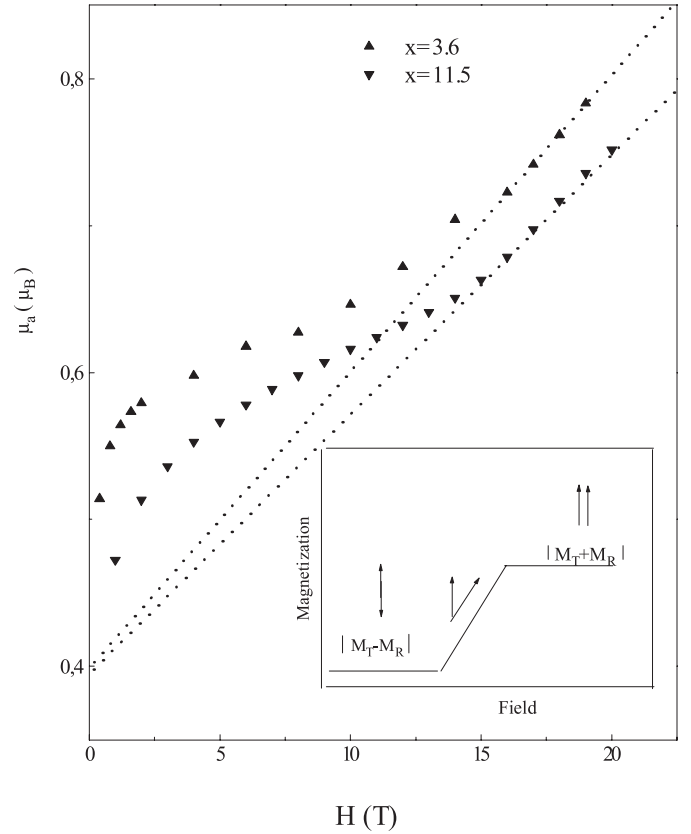


Fig. 5. Field dependence of the magnetic moment of the alloys for two concentrations: $x = 3.6$, and $x = 11.5$. The inset shows the schematized curve for a ferrimagnetic system containing two magnetic sublattices.

Table 3. Values of calculated and experimental molecular field coefficients.

x	n_{RT}^{cal}	n_{RT}^{exp}
3.6	44.8	49.5
5.5	46.5	-
7.6	51.9	-
11.5	52.8	55.3

and high fields the magnetizations, corresponding to the saturated state, are equal to $|M_T - M_R|$ and $|M_T + M_R|$, respectively. In our case the high-field saturated state (the forced ferromagnetic state) was not reached, and needs fields higher than 20 T to be established. Values for the coefficient n_{RT} derived from the slope of the magnetization curve in the high-field region appear in Table 3.

The exchange coupling parameter J_{RT} , between the $4f$ spins and its $3d$ spin surroundings can be calculated directly from n_{RT} with the help of the following relation

$$J_{RT} = g_R N_T n_{RT} \mu_B^2 / (g_R - 1) z_{RT} \quad (6)$$

where N_T is the number of $3d$ atoms per unit of mass, and z_{RT} is the number of T -neighbors of the R atom, which is assumed to be equal to 12: n_{RT} increases with the Ho concentration which may be related to a variation of the

strength of the $3d-4f$ exchange with Ho concentration. In Er-Co-B [2] and Fe-Ho-B [10] alloys, this coefficient remains constant until reaching the magnetic compensation and then increases. Moreover, n_{RT} for the alloys studied is greater than that obtained for Fe-Ho-B alloys [10] (Tab. 2).

4 Conclusion

We have studied magnetization behavior of amorphous $\text{Co}_{80-x}\text{Ho}_x\text{B}_{20}$ alloys, for which a magnetic compensation occurs at about $x = 8$. Co and Ho spins order antiferromagnetically and this coupling breaks at sufficiently high fields. The Co moment remains practically constant until the concentration of magnetic compensation ($x \leq 8$) and then shows a decrease. The various exchange integrals, $J_{\text{Co-Co}}$ and $J_{\text{Co-Ho}}$ have been calculated using the mean field theory. $J_{\text{Co-Ho}}$ shows a very slight increase, and $J_{\text{Co-Co}}$ remains practically constant for $x < 8$, and then shows an increase. We have also evaluated the molecular field coefficient, n_{RT} , which values are rather higher than those observed for $\text{Fe}_{82-x}\text{Ho}_x\text{B}_{18}$ alloys.

References

1. R.W. Cochrane, R. Harris, M.J. Zuckermann, *Phys. Rev.* **48**, 1 (1978)
2. K.J. Radwanski, J.J.M. Franse, R. Krishnan, H. Lassri, *J. Magn. Magn. Mater.* **119**, 221 (1993)
3. J.J. Rhyne, J.H. Schelleng, N.C. Koon, *Phys. Rev. B* **10**, 4672 (1974)
4. P. Chaudhary, J.J. Cuomo, R.J. Gambino, *IBM J. Res. Dev.* **17**, 66 (1973)
5. R. Krishnan, H. Lassri, *Sol. Stat. Commun.* **69**, 803 (1989)
6. M. Slimani, M. Hamedoun, M. Tlemçani, H. Arhchoui, S. Sayouri, *Physica B* **240**, 372 (1997)
7. P. Hansen, in: *Handbook of Magnetic Materials*, edited by K.H.J. Buschow (North Holland, Amsterdam, 1991), Vol. 6, p. 324
8. R.C.O. Handly, M.O. Sullivan, *J. Appl. Phys.* **52**, 1841 (1981)
9. X. Oudet, *J. Magn. Magn. Mater.* **65**, 99 (1987)
10. A. Kaal, O. El Marrakechi, S. Sayouri, M. Tlemçani, *Physica B* **325**, 98 (2003)
11. J.M.D. Coey, *J. Appl. Phys.* **49**, 1646 (1978)
12. R. Hasegawa, B.E. Argyle, L.J. Tao, *AIP Conf. Proc.* **24**, 110 (1975)
13. R. Hasegawa, *J. Appl. Phys.* **45**, 3109 (1974)
14. V.G. Harris, K.D. Aylesworth, B.N. Das, W.T. Elam, N.C. Koon, *Phys. Rev. Lett.* **69**, 315 (1995)
15. K. Yamauchi, T. Mizoguchi, *J. Phys. Soc. Jpn* **39**, 541 (1975)
16. K. Yano, Y. Akiyama, K. Tokumitsu, E. Kita, H. Ino, *J. Magn. Magn. Mater.* **214**, 217 (2000)
17. M. Slimani, M. Hamdoun, A. Itri, H. Lassri, R. Krishnan, *J. Magn. Magn. Mater.* **163**, 349 (1996)
18. S. Ishio, N. Obara, S. Nagami, T. Miyazaki, T. Kanamori, H. Tange, M. Goto, *J. Magn. Magn. Mater.* **119**, 271 (1993)
19. J.F. Herbst, J.J. Croat, *J.A.P.* **55**, 3032 (1984)
20. H. Rui-Wang, Z. Zhong-Wu, H. Bin, K. Jian-Dong, X.K. Un, Y.C. Chuang, *J. Magn. Magn. Mater.* **119**, 180 (1993)
21. R. Verhoef, R.J. Radwanski, J.J.M. Franse, *J. Magn. Magn. Mater.* **89**, 176 (1990)